



# Geophysical signatures of the Au-Ag mineralization in the Jersey Valley property, north-central Nevada, USA

Karl Kwan<sup>1</sup>, Paul Anderson<sup>2</sup>, and Riaz Mirza<sup>1</sup>

<sup>1</sup>Simcoe Geoscience Limited, Stouffville, Ontario, Canada

<sup>2</sup>Abacus Mining & Exploration Corporation

## Abstract

In the future, Time Domain Induced Polarization (IP) surveys will continue to play a growing role in the search for mineral deposits under-cover and at greater depths (> 500 m). The standard deliverable products for IP surveys are 2D/3D chargeability and resistivity inversion models. In many cases, the chargeability anomalies can be used to target potential disseminated sulphide mineralization directly. However, disseminated sulphide mineralization/deposit can occur in conductive as well as resistive settings. The Metal Factor (MF) is a more appropriate IP parameter in moderately conductive settings to identify targets. In this contribution, we will demonstrate the effectiveness of using the MF to identify epithermal low sulphidation Au-Ag mineralization in the Jersey Valley properties in an active geothermal setting near north-central Nevada in USA.

## Introduction

Schodde (2020) showed that geophysics accounts for nearly 22% of all prospect-scale (drilling stage) discoveries, and it can be expected to play a growing role in discovering new mineral deposits under-cover and at greater depths (>500 m). We believe that the success of geophysics at the prospect-scale can be credited largely to the ground/borehole IP/EM methods used to follow-up the airborne magnetic and electromagnetic (EM) anomalies.

In general, the standard final deliverables of a ground Induced Polarization (IP) survey are chargeability and resistivity inversions and, in many cases, for example, in the exploration for porphyry copper systems, the chargeability anomalies correlate directly with disseminated sulphide bodies and can be used to site the test drillholes. However, high chargeable responses can be found in conductive as well as resistive hosts, and in some cases the chargeability and resistivity inversions have proved to be inadequate in identifying the sought mineral targets. Müller, Kwan & Riaz (2021) have shown that the metal factor (MF) is more effective in the search for vein and breccia hosted high sulphidation polymetallic Au-Ag mineralization in the Stikinia terrane in northwestern BC, Canada.

The MF in IP was first introduced by Marshall & Madden (1959) to highlight chargeable zones in conductive host. MF correlates well with the metallic mineral content (Hallov, 1964). In frequency-domain IP, MF is defined as the ratio of the percent frequency effect (*PFE*) over the resistivity multiplied by 2000 (Sumner, 1979). In the time-domain IP, the *PFE* is replaced by the chargeability *m*, and for  $PFE \ll 1$ ,  $m \approx PFE$ . Therefore, in the time-domain IP, the MF is defined as the ratio of the chargeability *m* in (mV/V) and the resistivity  $\rho$  in (Ohm-m) multiplied by 2000, i.e.,

$$MF = 2000 * (m/\rho) \text{ in (mS/m)}. \quad (1)$$

The MF helps to increase the signal-to-noise ratio between the effect of well mineralized zones and the effect of only slightly mineralized zones, but it also favors the rocks having conductive electrolytes in the pores, and therefore it is not so useful when dealing with clays (Marshall & Madden, 1959 and Sumner, 1979).

The Jersey Valley property, acquired by Abacus Mining and

Exploration Corp. (Abacus) in 2019 under a 15-year lease and centered near 40° 10' 17" N and -117° 28' 35" W, approximately 69 kilometers southwest from Battle Mountain, Nevada (Fig. 1). Access to the Jersey Valley project is by paved road from Battle Mountain.



Figure 1: The location of the Jersey Valley property in north-central Nevada.



## Low Sulphidation Epithermal Gold Deposits in Nevada

The northern Great Basin of Nevada hosts world-class Miocene to early Pliocene low sulphidation (LS) epithermal gold deposits, e.g., Round Mountain, Mule Canyon, and Midas. Historical Production from those deposits exceeded 50 Moz Au (ca. 1996, John, 2001). World-class LS epithermal gold districts include Comstock Lode, Tonopah, Goldfield and Aurora (John, 2001). In the Comstock Lode district of Western Nevada, Mesozoic metasedimentary and volcanic rocks are overlain by Oligocene to Miocene ash-flow tuffs, and a thick sequence of middle Miocene and andesitic volcanic rocks and intrusions host the bulk of the hydrothermal alteration and ore deposits (Hudson, 2003). Epithermal deposits form over the temperature range from 160°C to 270°C (Hedenquist et al., 2000), from surface to depths up to 1.5 km (Taylor, 2007). Two main styles of epithermal gold deposits are the low sulphidation and high-sulphidation (HS) (White & Hedenquist, 1995). The precipitation of bisulphide-complexed metals such as gold is driven mainly by boiling (Fig. 2), resulting in many related features such as gangue-mineral deposition of quartz, adularia, and bladed calcite/quartz in LS deposits.

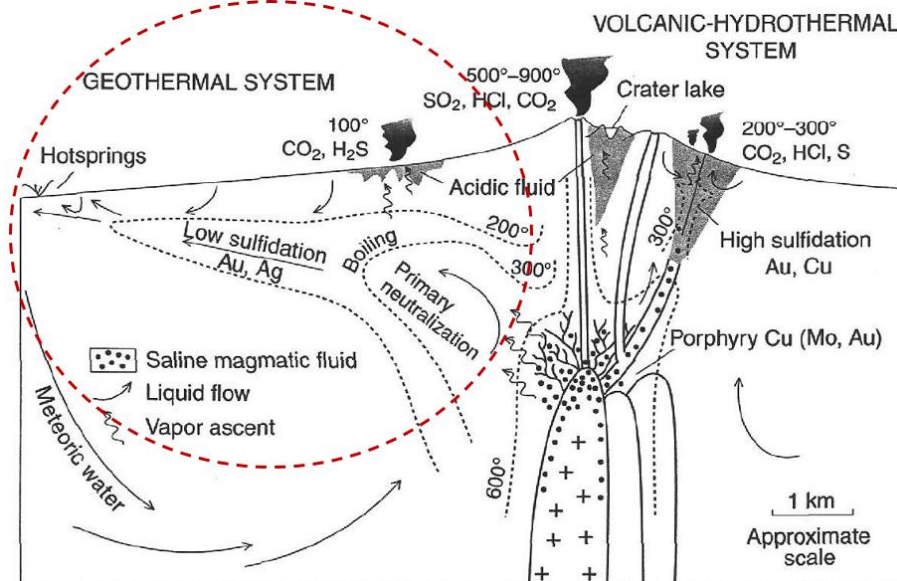


Figure 2: Schematic illustrations of volcanic-hydrothermal and geothermal systems and the respective environments for LS and HS epithermal deposits (from Hedenquist et al., 2000); the dashed circle (burgundy color) highlights the geothermal LS epithermal style mineralization.

## Alpha IP™ System

The Alpha IP™ – a 2D/3D Wireless Time Domain Distributed System is the world first wireless Induced Polarization system, where a minimum amount of wire is being used and can be expanded to as many channels and eliminates the concept of limited “n” values. Alpha IP™ provides full waveform data with 24-bit digital sampling and advanced signal processing. The chargeability and resistivity components provide an excellent means of delineating target mineralization.

In resistivity surveying, information about the subsurface distribution of electrical conductivity is obtained by examining how currents flow in the earth. DC (direct current) resistivity methods involve injecting a steady state electrical current into the ground and observing the resulting distribution of potentials (voltages) at the surface or within boreholes.

Chargeability is a physical property that is related to resistivity. The module about DC resistivity shows that potentials measured in a DC resistivity survey can be related to charges that accumulate when current is made to flow. However, when the transmitter current is switched off, the measured voltage may take up to several seconds to reach zero. Similarly, when the current is switched on, there may be a finite time taken for the voltage to reach a steady state value. In other words, current injected into the ground causes some materials to become polarized. The phenomenon is called induced polarization, and the physical property that is measured is usually called chargeability, which quantifies the material's capacity to retain charges after a forcing current is removed. The following figure illustrates the measurable effect.

Time domain IP is a rather complex phenomenon but easy to measure. When a voltage applied between two electrodes is abruptly interrupted the electrodes used to monitor the voltage do not register an instantaneous drop to zero but rather records a fast-initial decay followed by a slower decay. This phenomenon is known as IP (Fig. 3). The technique is mostly concerned with measuring



Disseminated sulphides have strong IP responses. Clay minerals may also produce significant IP responses. The IP technique is often used to distinguish between clay and for example water saturated media which have similar resistivities but different chargeability.

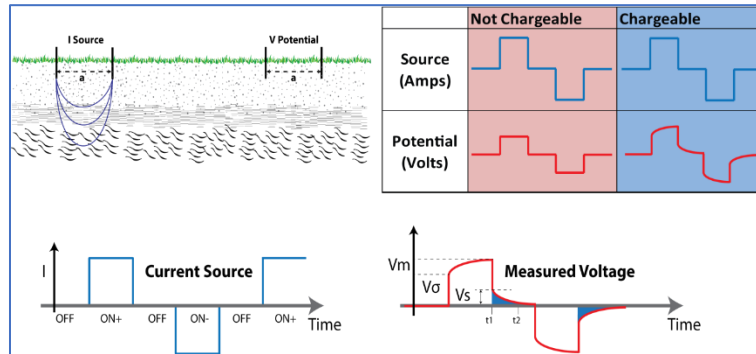


Figure 3: Example of Time Domain IP Measurement Sequence and Parameters.

Typical 2D IP surveys use the so-called distributed system, using wired or wireless receivers with full waveform recording, with the simultaneous deployment of unlimited receiver dipoles along any length of profile using 25/50/100/200 m long dipoles. Each receiver is fully independent, with its power source, GPS synchronization, and memory for data recording. The post-survey processing includes quality check and the extraction of resistivity and chargeability parameters at each plot point of a pseudo section, all carried out in the time-domain. After that, 2D inversions of the resistivity and chargeability parameters are produced as final deliverables, and they form the database for subsequent geophysical interpretation with the ultimate objective of identifying potential mineralization targets and siting of test drillholes.

Alpha IP™ system can be deployed in many configurations – Pole-Pole, Dipole-Dipole, Pole-Dipole, Gradient Array, and Simcoe’s Dipole-Pole-Dipole Array. The accuracy of dip and strike positions of structures is decreased (side shift) if only pole-dipole (PDR) or (PDL) is used, combining the PDR and PDL overcome misleading positions of structures, so the choice of Simcoe’s Dipole-Pole-Dipole configuration is highly recommended (Fig.4).

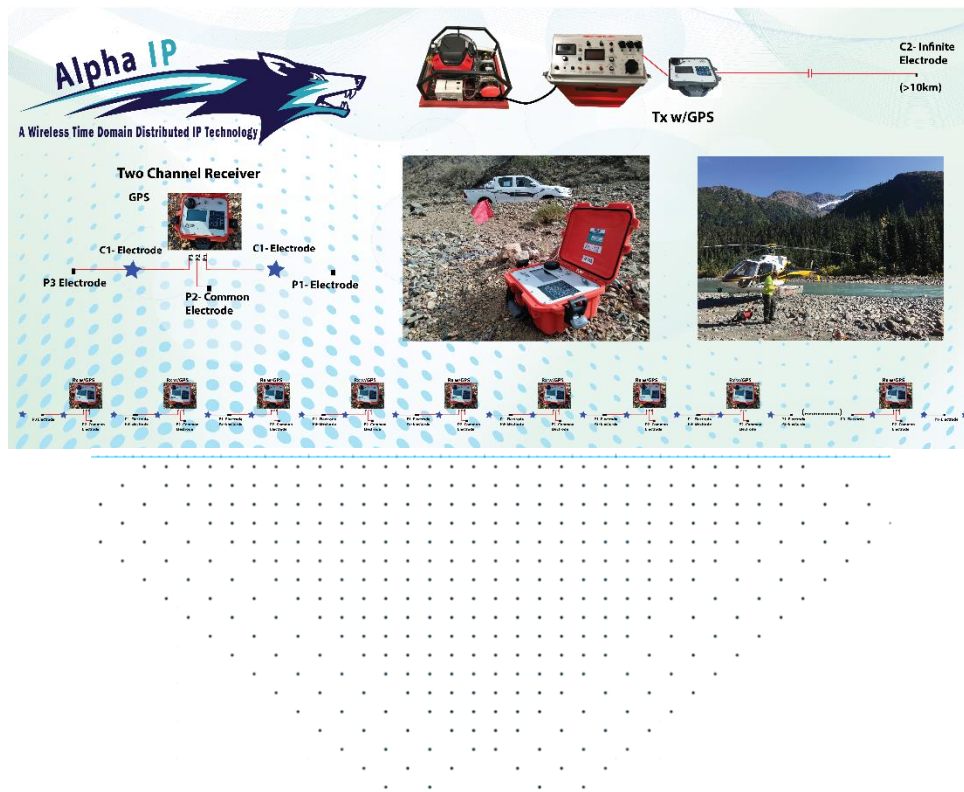


Figure 4: Alpha IP Dipole-Pole-Dipole Schematic Spread Setup with Current Injection Offset



# Jersey Valley Property

## IP Surveys

The 2020 high-resolution time domain IP survey totaled 14 line-kilometres and was designed to bracket the four IP lines, L0, L2 to L4, acquired in 2005 (Fig. 5). Three 2020 IP lines, L2020\_1 to L2020\_3, are selected for this study. The 2005 IP survey was laid out to penetrate to a depth of approximately 150 metres, while the new survey was designed to reach over 400 metres in depth.

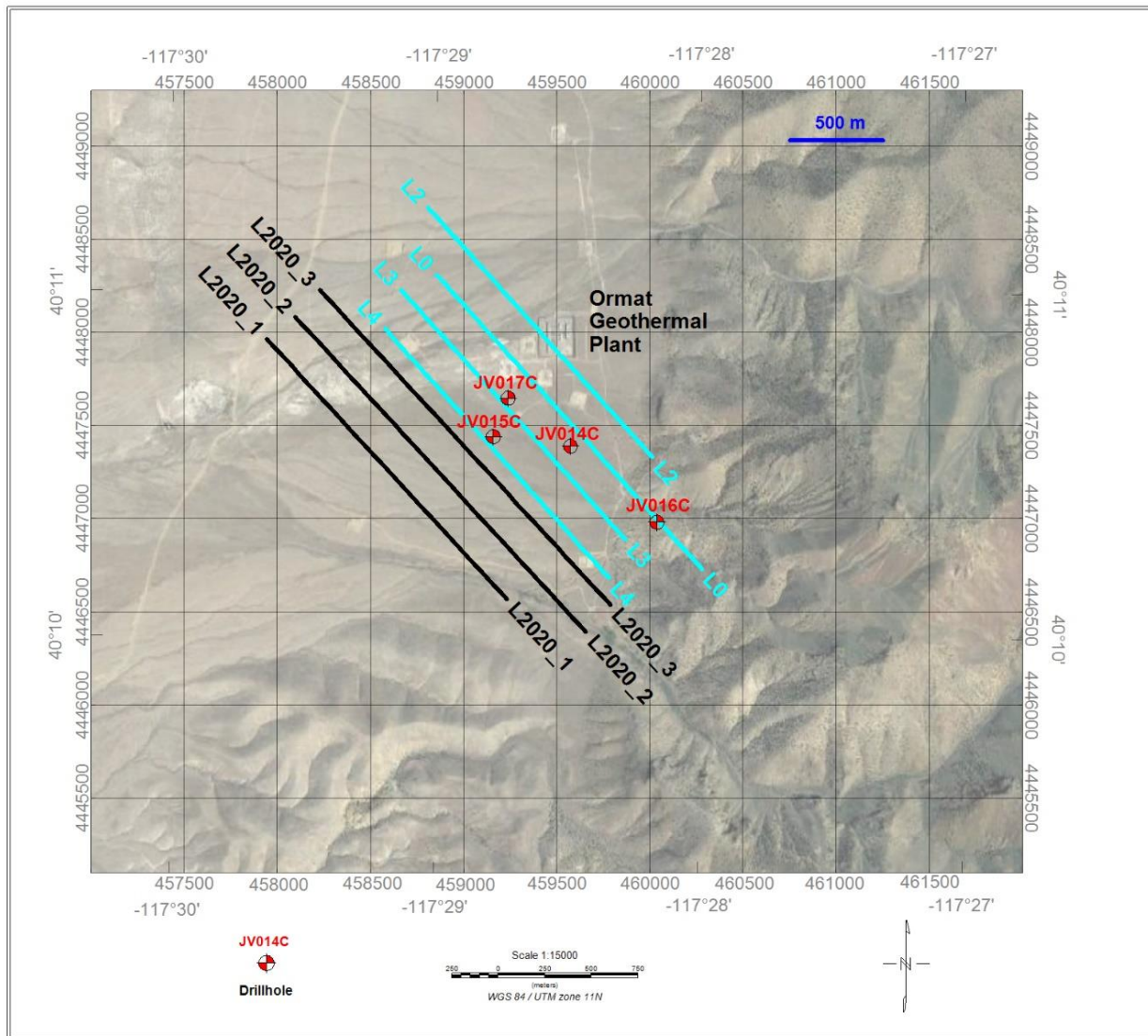
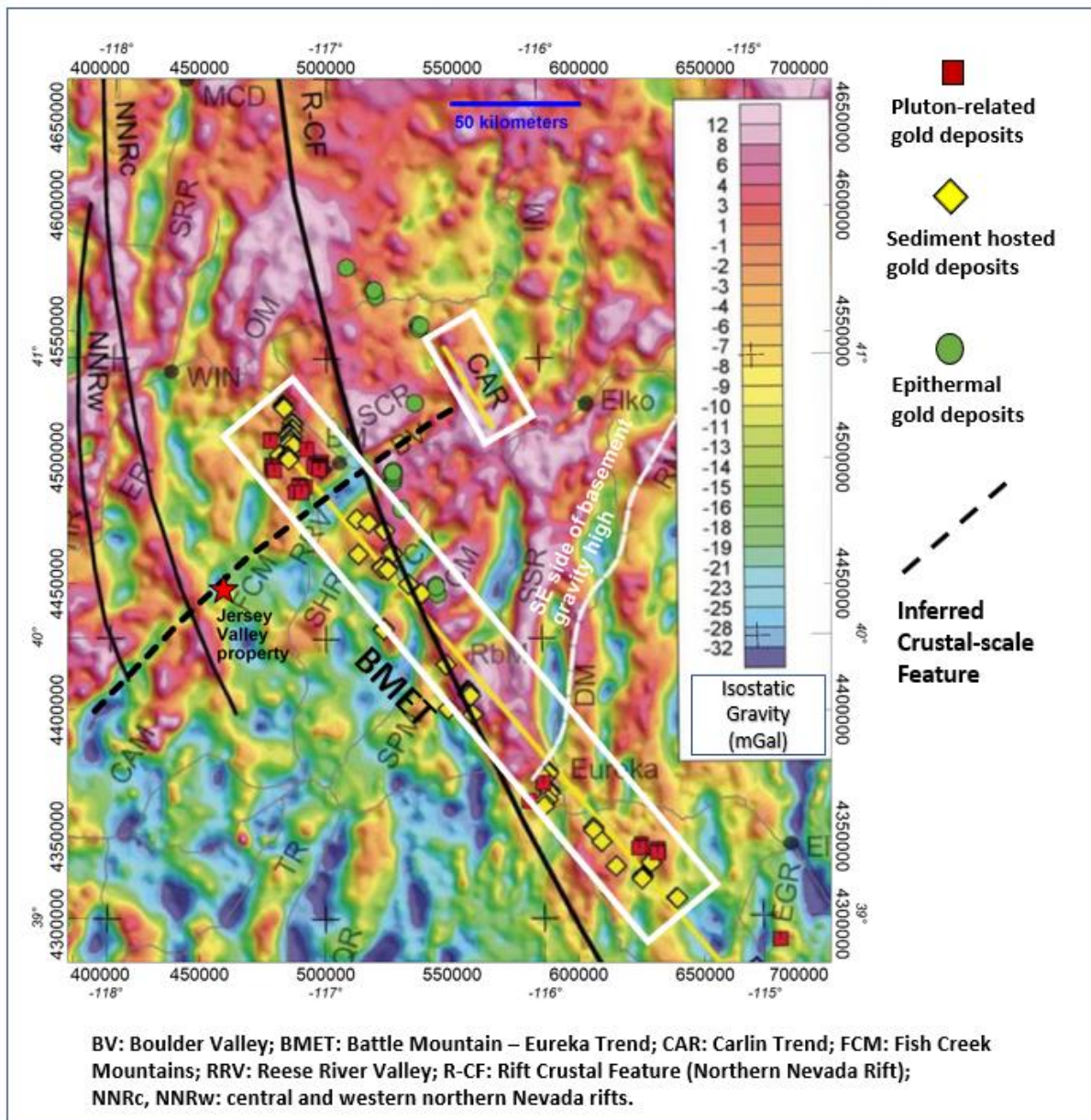


Figure 5: The location of IP survey lines over the Google Earth image; L0 to L4 lines were acquired in 2005 and provided by Abacus; L2020\_1 to L2020\_3 lines were acquired in 2020.

The isostatic gravity data of north-central Nevada (from Ponce & Glen, 2008) are shown in Fig. 6. The isostatic gravity results from the correction of the gravitational effect of low-density mountain roots, after Bouguer correction. A possible crustal-scale feature cross-cutting the Battle Mountain – Eureka Trend (BMET) is inferred from the isostatic gravity map. This feature starts from just west of the Carlin Trend (CAR), traverses along the Boulder Valley and Reese River Valley and the Fish Creek Mountains in the SW direction and passes through the Jersey Valley property. This feature seems to be related to relatively low-density felsic rocks and could be a regional and controlling structure for the emplacement of granitic plutons, including the Jersey stock, and potential intrusion-related epithermal gold, gold skarn and sediment hosted gold deposits.



**BV: Boulder Valley; BMET: Battle Mountain – Eureka Trend; CAR: Carlin Trend; FCM: Fish Creek Mountains; RRV: Reese River Valley; R-CF: Rift Crustal Feature (Northern Nevada Rift); NNRC, NNRw: central and western northern Nevada rifts.**

Figure 6: Isostatic gravity data, Carlin and Battle Mountain – Eureka trends, known pluton-related, sediment hosted and epithermal gold deposits (from Ponce & Glen, 2008); an inferred crustal-scale feature trending nearly SW-NE passes through the Jersey Valley property.

### Local Geology and Mineralization

The district where the Jersey Valley property is situated is on the western edge of the rifted North American craton near a lithospheric terrane boundary, northern Nevada Rife (NNR), with accreted oceanic terranes to the west (Bonner, 2019). The oldest exposed unit in the Jersey Valley area is the allochthonous Mississippian-Permian Havallah formation of metamorphosed marine sediments (Silberling & Roberts, 1962).

The western half of the Jersey Valley area is underlain mostly by Quaternary alluvium (Qal) and older alluvium and volcaniclastic sediments (Qoal), Fig.7. The eastern half of the Jersey Valley property is dominated by the Jersey Stock (Tgd), a granodiorite to diorite porphyry. The geology of the area north of the Jersey stock consists of mainly the granodiorite to diorite intrusives, dykes and breccia intercalated with limestone, sandstone, and chert.

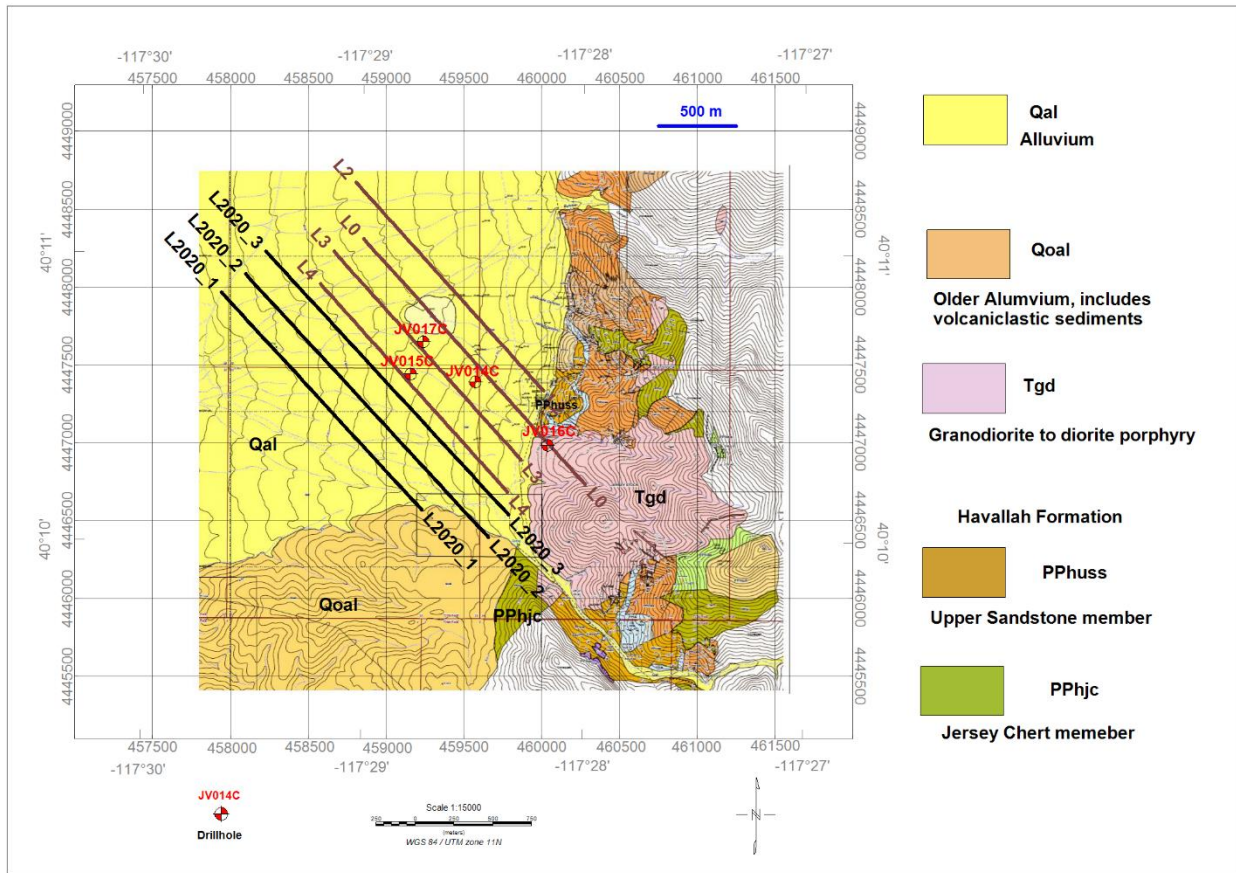


Figure 7: Local geology of the Jersey Valley property.

The mid-Miocene epithermal gold deposits have been shown to correlate spatially with the Northern Nevada Rifts (NNRs) (Ponce & Glen, 2002). The 15 MW Ormat Jersey Valley geothermal power plant is located in the Jersey Valley property, which has good potential for epithermal gold mineralization in an active geothermal environment similar to the Taupo volcanic zone in New Zealand, Krupp & Seward (1987). Nearby deposits include the Phoenix/Fortitude mine complex (a gold skarn with approximately 14 Moz gold plus significant Ag and Cu past production and a proposed mine life to 2063) and the Cove/McCoy Mine (a Carlin-type gold and polymetallic mineralization deposit with 3.4 Moz gold and 110 Moz Ag past production, Bonner, 2019).

According to Corbett (2002), LS epithermal Au-Ag deposits can be divided into two groups: those generated mainly from magmatic source rocks (arc low sulphidation), and those from circulating geothermal fluid sources (rift low sulphidation). The LS adularia-sericite epithermal Au-Ag systems belong to the rift low sulphidation type and they are dominated by gangue mineralogies derived from meteoric water rich circulating fluids, typically formed in rift settings (Corbett, 2002).

Because the epithermal gold deposits are highly variable in form, ranging from quartz veins to disseminated, and are in a wide variety of geological settings, their geophysical signatures are therefore can be complicated (Irvine & Smith, 1990). If the potential disseminated epithermal gold mineralization in the Jersey Valley property belongs to the LS type with pyrite as the dominant sulphide mineral, then its general geophysical expression will be moderately chargeable and moderately conductive.



### Ground Magnetic Data

The ground Reduced To Pole (RTP) magnetic data from the Jersey Valley property (provided by Abacus) are shown in Fig. 8. The strong RTP anomalies coincide with the Jersey Valley stock. The inferred faults/contacts are also shown. The area covered by the IP liens shown weak to moderate magnetic responses. There is a moderately strong magnetic anomaly in the ground in the middle part of L2020\_1 to L2020\_3, possibly correspond to a deeper magnetic source.

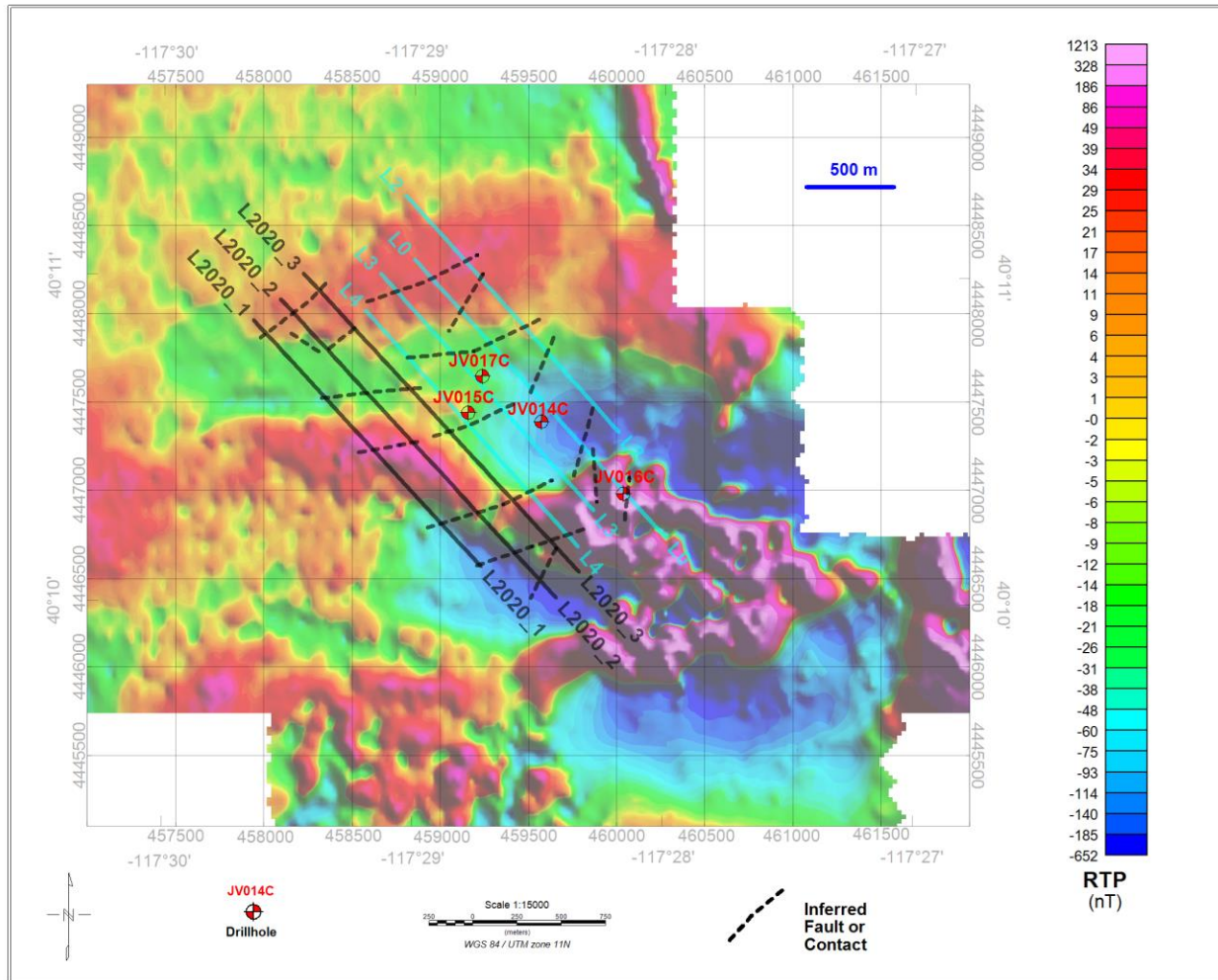


Figure 8: The ground RTP data of the Jersey Valley property (provided by Abacus).

### Interpretation of the IP data

The L0 chargeability, resistivity, and MF sections are shown in Fig.9. The hole traces of past drillholes 06JV014C and 0CJV016C are displayed in the chargeability and resistivity sections as well. The drillhole 06JV014C was collared within the northeast part of JV-1 (see Fig. 12) and drilled to the southeast, but it tested a weaker anomaly and missed a stronger, slightly deeper anomaly. Despite this, the hole intersected 1.18 g/t silver over 13.1 m near the top and then 0.19 g/t gold over 13.4 m within a slightly wider intercept of 2.36 g/t Ag over 16.5 m near the end of the hole.

The MF data is effective in reducing the influence of conductive anomalies without strong chargeability associations, for example, the conductive anomaly in the NW part of L0 in the resistivity section. The MF highlights the strong conductive and chargeable anomaly (JV\_1) in the middle part of the line.

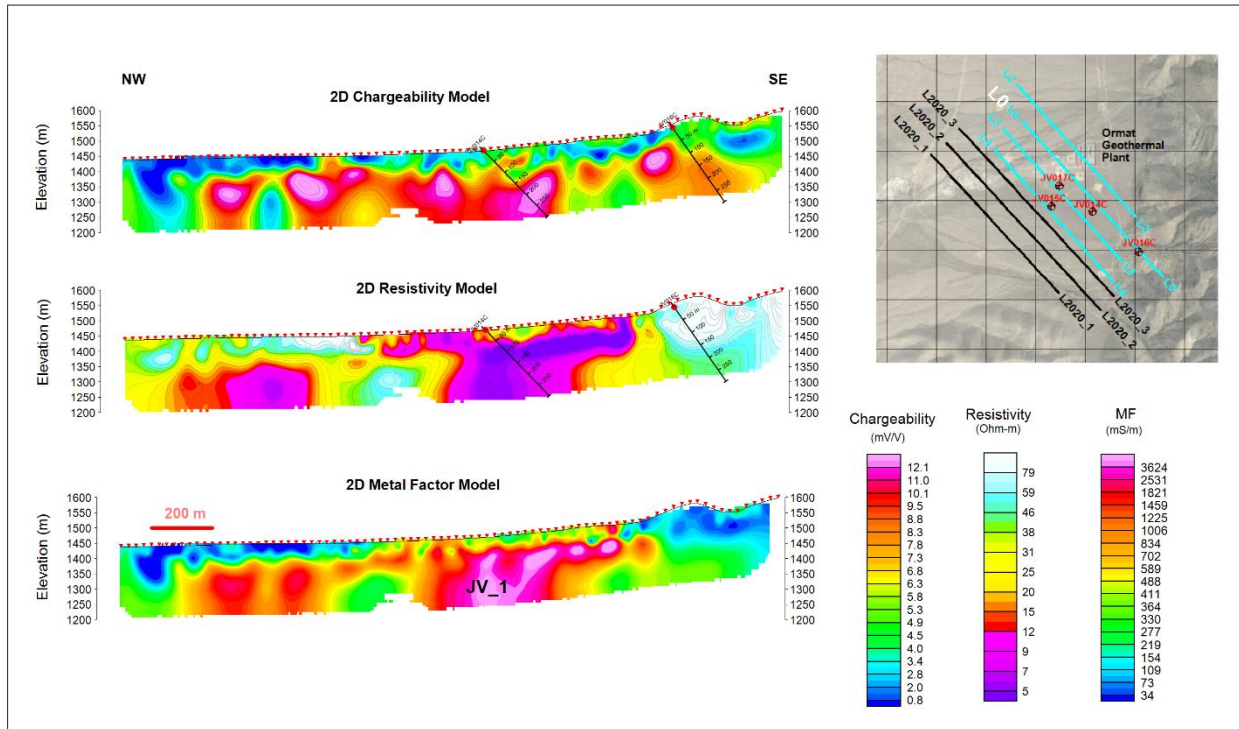


Figure 9: L0 2D chargeability, resistivity, and MF sections, drillhole traces and the selected target JV\_1 (see Fig. 12).

The L3 chargeability, resistivity and MF sections are shown in Fig. 10. The past drillhole 06JV017C, drilled to the northwest, which assayed narrow zones of anomalous gold and silver throughout, and then 0.18 g/t gold and 2.98 g/t Ag over 29.87 m. at the end of the hole. To the NW of the drillhole, there is a strong chargeability anomaly in a relatively resistive zone near the surface, possibly due to a sinter. The target JV\_1 is mapped very well by the MF data.

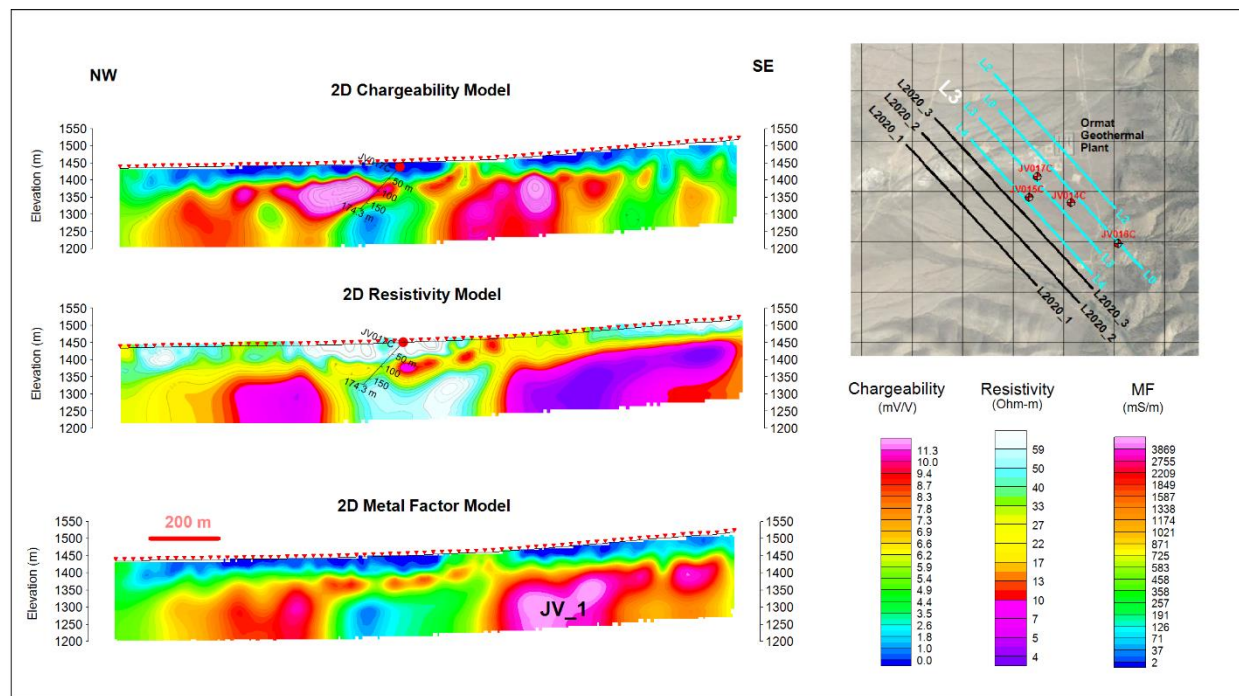


Figure 10: L3 2D chargeability, resistivity, and MF sections, drillhole traces and the selected target JV\_1 (see Fig. 12).



L2020\_2 chargeability, resistivity, and MF sections are displayed in Fig. 11. The target JV\_2 is mapped very well by the MF data. Potentially, there could be a deep target to the SE of JV\_2.

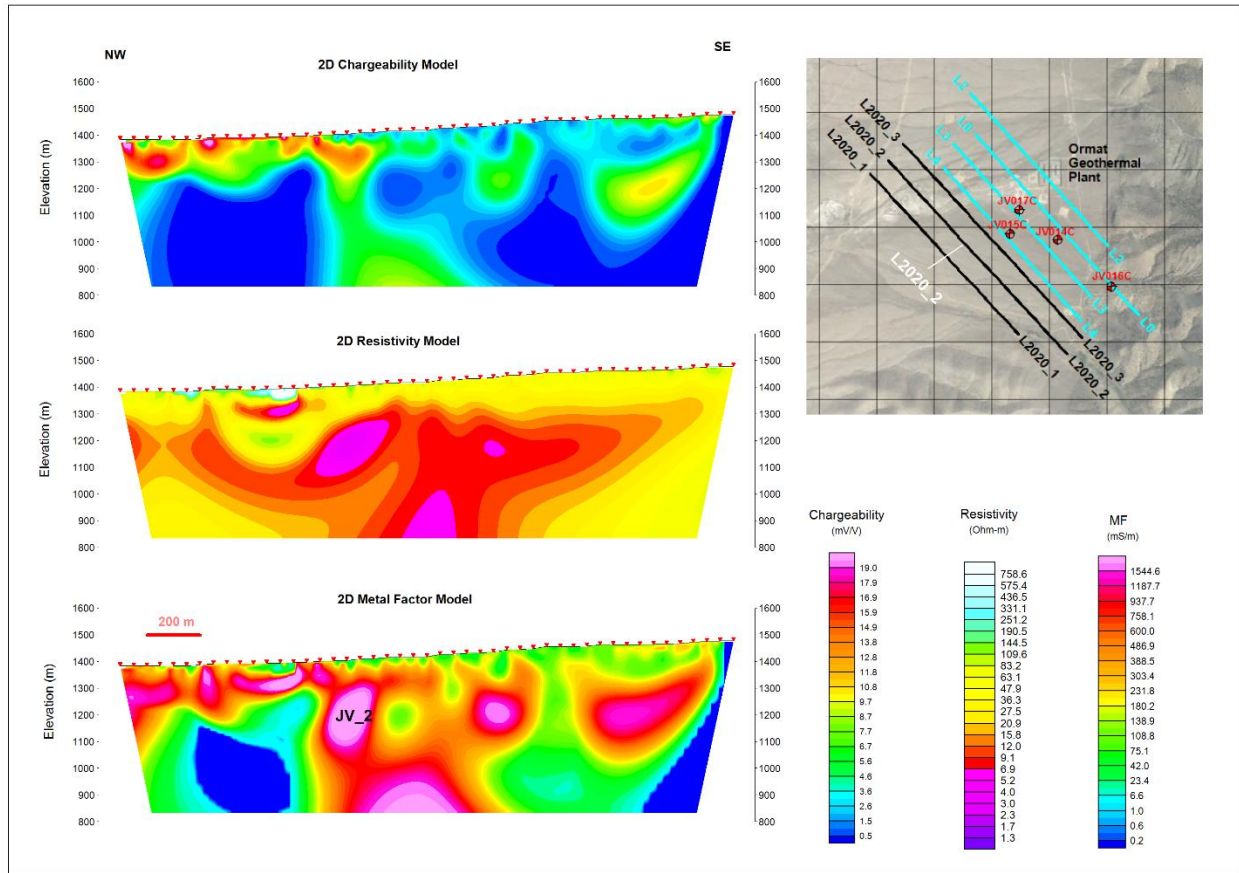


Figure 11: L2020\_2 2D chargeability, resistivity, and MF sections, drillhole traces and the selected target JV\_2 (see Fig. 12).

### Potential Epithermal Au-Ag Targets

2D inversion of the IP lines were merged and 3D chargeability, resistivity and MF voxels were created. The MF -200 m depthslice (with respect to the ground) is shown in Fig. 12, along with the two selected targets, JV\_1 and JV\_2. Part of the JV\_1 is tested by the drillhole 06JV014C. The target JV\_2 remains open to the south.

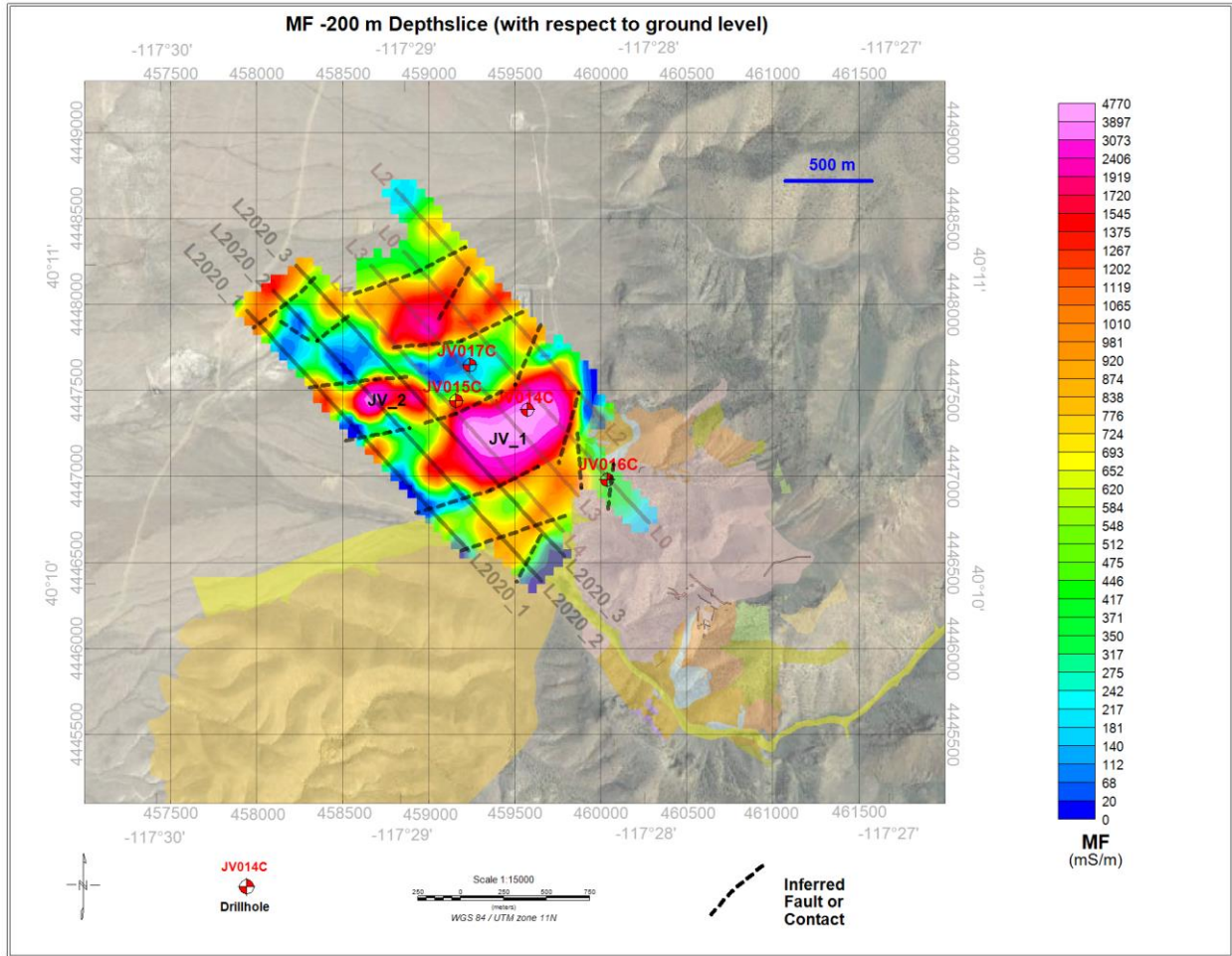


Figure 12: Selected sulphide targets over the MF -200 m depthslice.

## Discussions

A useful and diagnostic IP parameter that can be extracted from the time-domain IP survey is the relaxation time-constant  $\tau$  in the Cole-Cole model (Pelton et al. 1978) shown below.

$$\rho(\omega) = \rho_0 \left[ 1 - m \left( 1 - \frac{1}{1 + (i\omega\tau)^c} \right) \right]$$

$\rho(\omega)$ : frequency dependent resistivity in Ohm-m.

$\rho_0$ : low frequency asymptotic resistivity in Ohm-m.

$m$  ( $0 \leq m \leq 1$ ): dimensionless chargeability.

$\tau$ : relaxation time-constant in second.

$c$  ( $0 \leq c \leq 1$ ): frequency factor.

The chargeability  $m$  is related to the amount of polarizable material,  $\tau$  to the size of the polarizable grains, and  $c$  to the distribution of grain sizes, from non-uniform (0) to uniform (1).



The relaxation time-constant  $\tau$  alone or in combination with other Cole-Cole parameters, could be used potentially to differentiate the clay (generally fine-grained) from coarse-grained sulphides. The relaxation time-constant  $\tau$  has been shown to be potentially useful in the search for Archean greenstone-hosted gold in Ontario Canada by Müller, Kwan & Groves (2021).

The product of chargeability  $m$  and time-constant  $\tau$  can highlight chargeable zones with coarse-grained polarizable materials. A case is presented by Kwan & Müller (2020) to use  $m\tau$  to map the alteration halos around porphyry stocks at Mt Milligan, British Columbia Canada.

## Conclusions

Schodde (2020) pointed out that geophysics can be expected to play a growing role in the exploration for mineral deposits under cover and at greater depths (> 500 m). In order to make it happen, we geophysicists need to provide more relevant and effective geophysical products closely related to geology and mineralization.

In this contribution, we have demonstrated the effectiveness of the MF data in the exploration for potential low sulphidation epithermal Au-Ag mineralization in an active geothermal setting in the Jersey Valley property, north-central Nevada, USA. This case also calls for geophysicists to produce more relevant and appropriate products and be more innovative.

## Acknowledgments

We like to thank Abacus Mining and Exploration Corporation for granting the permissions to publish the geophysical data from the Jersey Valley Project in Nevada, USA.

## References

- Bonner, W.M., 2019. Spatial and temporal relationship between Carlin-Style gold and polymetallic mineralization at the Deep Cover Gold-Silver deposit, Lander County, Nevada, unpublished M.Sc. thesis, University of Nevada, Reno.
- Corbett, G., 2002. Epithermal gold for explorationists, *AIG Journal – Applied geoscientific practice and research in Australia*, 1-26.
- Hallof, P.G., 1964. A comparison of the various parameters employed in the variable-frequency induced-polarization method, *Geophysics*, **29**:3, 425-433.
- Hedenquist, J.W., Arribas, A., and Gonzalez-Urien, E., 2000. Exploration for epithermal gold deposits, *SEG Reviews*, **13**, 245-277.
- Hudson, D.M., 2003. Epithermal alteration and mineralization in the Comstock district, Nevada, *Economic Geology*, **98**, 367-385.
- Irvine, R.J. and Smith, M.J., 1990. Geophysical expression for epithermal gold deposits, *Journal of Geochemical Exploration*, **36**, 375-412.
- John, D.A., du Bray, E.A., Henry, C.D. and Vikre, P.G., 2015. Cenozoic magmatism and epithermal gold-silver deposits of the southern ancestral Cascades arc, western Nevada and eastern California, in Pennell, W., and Garside, L.J., eds., *New concepts and discoveries: Geological Society of Nevada 2015 Symposium Proceedings*: Reno, Nevada, Geological Society of Nevada, 611-645.
- John, D.A., Hofstra, A.H., Fleck, R.J., Bummer, J.E., and Saderholm, E.C., 2003. Geologic setting and genesis of the Mule Canyon low-sulphidation epithermal gold-silver deposit, north-central Nevada, *Economic Geology*, **98**, 425-463.
- John, D.A., 2001. Miocene and Early Pliocene epithermal gold-silver deposits in the northern Great Basin, Western United States: Characteristics, distributions, and relationship to magmatism, *Economic Geology*, **96**, 1827-1853.
- Johnston, M.K., Thompson, T.B., Emmons, D.L. and Jones, K., 2008. Geology of the Cove Mine, Lander County, Nevada, and a genetic model for the McCoy-Cove hydrothermal system, *Economic Geology*, **103**, 759-782.
- Krupp, R.E. and Seward, T., 1987. The Rotokawa geothermal system, New Zealand: An active epithermal gold-depositing environment, *Economic Geology*, **82**, 1109-1129.
- Kwan, K. and Müller, D., 2020: Mount Milligan alkalic porphyry Au-Cu deposit, British Columbia, and its AEM and AIP signatures: Implications for mineral exploration in covered terrains, *Journal of Applied Geophysics*, **180**, 104131.
- Marshall, D.J. and Madden, T.R., 1959. Induced polarization, a study of its causes, *Geophysics*, **24**, 790-816.



- Müller, D., Kwan, K. and Groves, D.I., 2021. Geophysical implications for the exploration of concealed orogenic gold deposits: A case study in the Sandy Lake and Favourable Lake Archean greenstone belts, Superior Province, Ontario, Canada, *Ore Geology Reviews*, **128**, 103892.
- Pelton, W.H., Ward, S.H., Hallof, P.G., Sill, W.R., Nelson, P.H., 1978. Mineral discrimination and removal of inductive coupling with multi-frequency IP. *Geophysics*, **43**, 588–609.
- Ponce, D.A. and Glen, J.M.G., 2008. A prominent geophysical feature along the northern Nevada rift and its geologic implications, north-central Nevada, *Geosphere*, **4** (1), 207-217.
- Ponce, D.A. and Glen, J.M.G., 2002. Relationship of epithermal gold deposits to large-scale fractures in Northern Nevada, *Economic Geology*, **97**, 3-9.
- Silberling, N. J. and Roberts, R. J., 1962. Pre-Tertiary Stratigraphy and Structure of Northwestern Nevada, in Silberling, N. J. and Roberts, R. J. (Eds.), *Pre-Tertiary Stratigraphy and Structure of Northwestern Nevada: Geological Society of America*, p0.
- Schodde, R., 2020. The challenges and opportunities for geophysics for making discoveries under cover; presented at the Canadian Exploration Geophysical Society (KEGS) PDAC meeting, March 3, 2020.
- Sillitoe, R.H. and Bonham, H.F., 1990. Sediment-hosted gold deposits: Distal products of magmatic-hydrothermal systems, *Geology*, **18**, 157–161.
- Sumner, J.S., 1979. The induced-polarization exploration method; in Peter J. Hood Ed *Geophysics and Geochemistry in the search for metallic ores; Geological Survey of Canada, Economic Geology Report 31*, 123-133.
- Taylor, B.E., 2007. Epithermal gold deposits, in Goodfellow, W.D., ed., *Mineral deposits of Canada: A synthesis of major deposit-types, district metallogeny, the evolution of geological provinces, and exploration methods: Geological Association of Canada, Mineral Deposits Division, Special Publication No. 5*, 113-139.
- White, N.C. and Hedenquist, J.W., 1995. Epithermal gold deposits: Styles, characteristics and exploration, *SEG Newsletter*, **23**, p.1, 9-13.